



TECHNICAL ARTICLE

Mechanical Performance Analysis of Offshore Platform Based on the Modified Generalized Constitutive Model of Time-Varying Corrosion-Damaged Steel

Lu Qiqi, Yang Yang, Sun Shuang, and Weng Yu

Submitted: 11 November 2022 / Revised: 24 February 2023 / Accepted: 4 March 2023 / Published online: 11 April 2023

Aiming at the limitation of section reduction method and multi-scale method to simulate corrosion-induced steel offshore platform, a generalized steel constitutive model was proposed considering the variability, randomness and locality of corrosion. To simulate possible corrosion scenarios, random corrosion treatment with different corrosion degrees was carried out on offshore steel specimens using electrochemical accelerated corrosion, and the relationship between laboratory corrosion specimens and platform corrosion components and the equivalent corrosion life of the specimens were obtained based on a time-varying model of platform corrosion thickness established by regression analysis of corrosion data from the platform. Monotonic tensile tests on specimens with different corrosion degrees were conducted to obtain the time-varying corrosion damage influence law of steel mechanical properties, based on R–O model of linear exponential time-varying corrosion loss, a generalized constitutive model for steel, with the aid of this model to push static pushover analysis of service platform, platform reserve strength and ductility time-varying corrosion influence law of reserves, the simulation of corrosion damage caused by steel offshore platforms in different service periods can be realized.

Keywords generalized constitutive model, mechanics performance, ocean platform, structural steel, variant-time corrosion

1. Introduction

The environment of steel marine engineering structures is generally relatively harsh, and most of the structures have been in service for a long time. The corrosion and corrosion acceleration effects caused by complex and diverse environmental effects are obviously more serious than other engineering structures. Corrosion forms in marine environments are not the same. According to the corrosion area, it can be divided into general corrosion and local corrosion. Uniform corrosion is relative to local corrosion, and its risk of corrosion is relatively small. According to the corrosion rate and material life, the corrosion tolerance can be set aside at the beginning of the design. Localized corrosion is confined to certain areas of corrosion occurring on metal surfaces, with uneven corrosion. In actual engineering, the corrosion effect of the overall platform is usually investigated by simulating uniform corrosion by the cross-section reduction method. This method cannot reflect the random distribution and local characteristics of corrosion. Modeling using solid or multi-scale methods will lead to problems such as heavy workload, complex analysis

Lu Qiqi, Yang Yang, Sun Shuang, and Weng Yu, School of Naval Architecture and Ocean Engineering, Dalian University of Technology, Liaoning, China. Contact e-mail: yyang@dut.edu.cn.

List of Symbols

β	Amplification coefficient (–)
ΔL	Displacement of the end of the specimen in the tensile test (mm)
ε	Strain (–)
μ	Ductility coefficient
ε_{el}	Elongation (–)
ε_n	Nominal strain (–)
ε_u	Ultimate strength strain (–)
ε_y	Yield strain corresponding to yield stress (–)
σ	Stress (MPa)
σ_n	Nominal stress (MPa)
σ_u	Ultimate strength (MPa)
σ_y	Yield Strength (MPa)
ϕ_{i1}	The mode coordinate of the i th floor (–)
A	Ground peak acceleration ($m \cdot s^{-2}$)
A_0	Sectional area of test section of intact specimen (mm^2)
d	Average diameter of the generated pits (mm)
D	External diameter of the pile (mm)
E_s	Young's modulus (GPa)
f_u	Ultimate strength (MPa)
f_y	Yield strength (MPa)
h_0	The bottom of the jacket platform (m)
I	Seismic precautionary intensity (–)
I_a	Equivalent seismic precautionary intensity (–)
k	A factor (–)
L_0	Length of test section (mm)
M_1^*	Product of effective mass (kg)
m_i	The mass of the i th floor (kg)
N	Number of floors of a structure (–)
r^2	Goodness of fit (–)

RSR	Reserve strength ratio (–)
t	Average depth of the generated pits (mm)
t_{test}	Corrosion time in laboratory (h)
T	Basic period of structure (s)
$T_{service}$	Years of service of the platform (year)
V_d	Design base shear (kN)
V_u	Ultimate base shear (kN)
S_m	The spectrum displacement of collapse point (m)
S_y	The spectrum displacement of yield point (m)

procedures, and difficult-to-converge calculations, which difficult to use in engineering. Therefore, it is valuable to propose a corrosion-damaged platform analysis method that not only reflects the true random corrosion characteristics of the platform, but also can be easily calculated.

In the analysis of the mechanical properties of corroded marine engineering structures, a reasonable and accurate corrosion model is very important. The multistage probabilistic phenomenological model (Ref 1) fully reveals the development process of pitting corrosion in marine engineering and provides important ideas for the study of pitting damage. However, it is difficult to obtain due to too many influencing factors. The Valor model (Ref 2) uses the inhomogeneous Poisson process to simulate the pitting initiation process and the inhomogeneous Markov process to simulate the pitting depth development, which is in good agreement with the actual engineering results. However, it is difficult to obtain the model because it needs to simulate a large number of measured results with random mathematical methods. In order to make the model simple and easy to use, the corrosion of steel offshore engineering structures is often simplified as uniform corrosion, and the corrosion depth becomes the only parameter for a constant degree of corrosion. The development of the corrosion depth can be expressed as a linear model or a nonlinear model that varies with exposure time (Ref 3, 4). The power function model and the Paik linear model are simple and easy to implement, but differ significantly from the marine corrosion behavior (Ref 5). Especially at the beginning of the study, the corrosion rate of the corrosion depth is usually assumed to be a constant value (Ref 6). However, the assumption of a constant corrosion rate was found to be quite different from the actual platform corrosion law. Based on the long-term measured data of actual ships, Soares and Garbatov (Ref 7) proposed a marine steel corrosion rate model based on the Weibull distribution. This model has also become the most commonly used model for calculating the deep corrosion rate of marine engineering structures. Paik et al. (Ref 8) regressed the above model based on a real ship that had been in service for 10 years and modified the model parameters. This model has been widely used in existing research and proved to be closer to the actual situation (Ref 9). Qin (Ref 5) proposed a corrosion rate model based on random distribution and seawater coupon test data; Melchers (Ref 10) established a segmented corrosion model of steel; the model has 6 statistical parameters, due to the need for a large amount of measured data to regress the above parameters, so the use of this model is somewhat difficult.

Corrosion will degrade the mechanical properties of steel, such as yield strength, ultimate strength, and ductile deformability, to varying degrees (Ref 11, 12). The bearing capacity, deformation capacity, and service life of corroded steel structures will be greatly reduced (Ref 13). Studies have found

that the high concentration of stress at local corrosion locations may be the main reason for the decrease in the ultimate bearing capacity of steel (Ref 14). Due to the complexity of the local stress concentration at the corrosion point and the resulting complexity of the change in the mechanical properties of the corrosion-damaged steel specimen or component, more researches tend to analyze the ultimate bearing capacity of structures based on pitting or uniform corrosion of components or structures. There are few researches on the change law of steel mechanical properties considering the influence of local corrosion and the corresponding damage mechanics model (Ref 15). For non-damaged steel, the R-O model is a classic theoretical model describing the stress–strain relationship of elastoplastic materials. However, the results of the R–O model are relatively high in the large strain stage (Ref 16). The constitutive model based on the R–O model can usually simulate the stress–strain relationship of the material at small strains more accurately, and the model is usually taken as a straight line at the large strain stage. Since more parameters are required to define the yield step in the constitutive model, such as the modified power law model (Ref 17) and the three-stage Asad Esmaeily and Yan Xiao model (Ref 18); most of the existing constitutive models do not include the yield platform. Generally, the analysis of the mechanical properties and bearing capacity of corroded steel structures is mostly based on the constitutive model of conventional steel. However, the characteristics of steel discontinuity and high local stress concentration caused by real corrosion cannot be reflected by the above-mentioned conventional steel constitutive model. And this just limits the authenticity of the overall analysis results of the corroded structure. Therefore, it is necessary and meaningful to propose and establish a steel generalized constitutive model that can be used for any corroded steel structure, considering the local characteristics of corrosion.

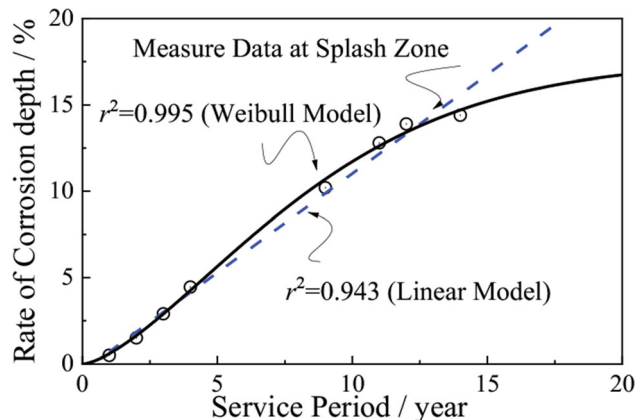
Based on the above analysis, a typical high-strength marine steel is selected, the seawater collected in the Bohai Sea is used as the corrosive medium, and the indoor electrochemical accelerated corrosion method is used to simulate the long-term seawater corrosion of the steel. According to the real platform measured corrosion data regression simulation platform long-term corrosion time change law, and combined with the change law of the corrosion thickness of the steel in the laboratory, to establish the relationship between the electrochemical corrosion time and the natural corrosion age. The monotonic tensile test was carried out on the steel plate specimens with different corrosion durations, and the time-varying corrosion influence law of steel mechanical properties was obtained, and based on R–O model, a generalized constitutive model of corroded steel is established. The constitutive correction model of steels with different corrosion years is introduced to simulate the influence of platform corrosion. The overall performance of the platform is analyzed, and its time-varying degradation law is investigated.

2. Time-Varying Corrosion Model of Offshore Platform

The Bohai No. 8 platform was built in the middle of the Bohai Sea in 1977. The platform has a design life of 20 years. Its measured data of the corrosion in the splash zone of the

Table 1 Corrosion measured data (wt.%)

Category	Rate of corrosive depth in different service years, %							
	1	2	3	4	9	11	12	14
Major brace	0.50	1.50	10.20	12.80
Diagonal chord	2.90	4.45	10.80	12.30	13.90	14.40

**Fig. 1** The fitting of the Weibull and linear models

platform are shown in Table 1. According to the measured corrosion data shown in Table 1, the time-varying model and expression of the corrosion thickness change rate in the splash zone of the platform are regressed, as shown in Fig. 1. Based on the random distribution characteristics of corrosion, the corrosion depth change rate in Table 1 is the average of the multi-point measurement results of the same component, which reflects the overall corrosion degree of the platform during a certain service period.

The Weibull model and the linear model are used to fit the measured corrosion depth data, respectively, and the Weibull model has a slightly higher goodness of fit. Regression to obtain the time-varying model of the average corrosion thickness of the platform splash zone in different service periods:

$$D(t) = 17.479(1 - e^{-0.107t^{1.507}}) \quad (\text{Eq 1})$$

where D is the corrosion depth; t is the corrosion time.

3. Steel Time-Varying Corrosion Test

3.1 Steel Material Properties and Specimen Size

In order to study the influence of the degree of corrosion on the mechanical properties of the platform structure, generalized constitutive models of corroded steels in different service periods need to be obtained. Therefore, the high-strength marine steel DH36 certified by the ABS classification society is used for the mechanical performance test of the corrosive steel. According to the test results provided by the manufacturer, the elastic modulus of the steel is 210GPa, the yield strength is 430 MPa, the ultimate tensile strength is 553 MPa, and the

elongation is 26%. The chemical element content of steel is shown in Table 2.

Since marine engineering structural components are mostly plates and thin-walled components, the test specimens are plates. The test piece is divided into test section, transition section, and clamping section, as shown in Fig. 2. According to the requirements of the ASTM standard (Ref 19), the detailed dimensions of the test piece are shown in Fig. 2.

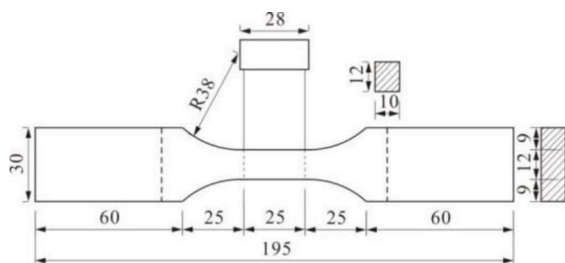
3.2 Electrochemical Accelerated Corrosion Test

To study the effect of long-term corrosion on the mechanical properties of steel, a corrosion simulation test of steel in a seawater environment must be conducted first. The laboratory corrosion method allows for accurately controlling the test conditions and can be completed in a shorter period. Laboratory corrosion usually includes electrochemical accelerated corrosion and mechanical drilling methods. Considering that the corrosion of steel is mainly electrochemical corrosion in the Marine environment, the electrochemical accelerated corrosion method is adopted to approximate the corrosion process of the above-mentioned real offshore platform steel (Ref 20). The electrochemical corrosion test device is shown in Fig. 3. Among them, the positive and negative electrodes of the constant current source are, respectively, connected to the inert electrode and the steel, the constant current is 4A, and the inert electrode and the steel specimen are placed in seawater collected from the Bohai Sea. A constant current is input to the test system, and the steel sample used as the anode is oxidized and dissolved. In order to ensure that the test piece is damaged in the test section, the end of the test piece is painted and wrapped with plastic tape for anti-corrosion protection. The steel specimens in seawater were energized for 1-8 h, and a total of 5 groups of corrosion specimens were obtained. The results of each group were averaged. The corrosion specimen parameters and photographs of the specimens are shown in Table 3.

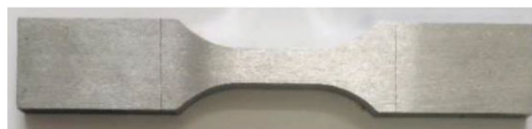
According to the corrosion thickness of the specimen and the above-mentioned time-varying model of corrosion thickness regressed from the measured data, the corrosion age of the laboratory electrochemical corrosion specimen in the real marine environment is inferred, as shown in Fig. 4. The corrosion ages of corrosion specimens in the real Marine environment obtained in Fig. 4 are shown in Table 3. In addition, according to Fig. 4, the corrosion depth rate of any service life can be obtained. For example, the corrosion depth rate of steel in service for 1-year, 5-year, 10-year, 15-year and 20-year steels is 0.585%, 5.668%, 11.730%, 15.214%, and 16.732%, respectively. Comparing the test and actual measurement results, the correlation between the laboratory corrosion time and the actual measurement period can be obtained, as shown in Fig. 5. The laboratory simulation law of corrosion can be further obtained. The surface of the corrosion test piece is

Table 2 The chemical composition of the hull structural plate (wt.%)

Element	Percentage	Element	Percentage	Element	Percentage	Element	Percentage
C	0.110	Si	0.37	Mn	1.180	P	0.013
Si	0.002	Cr	0.06	Al	0.034	Mo	0.001
Ti	0.012	Cu	0.06	Nb	0.016	Ni	0.010
V	0.006



(a) Specimen size



(b) A physical picture of the specimen Front view

Fig. 2 Details of standard tensile specimen (unit: mm)

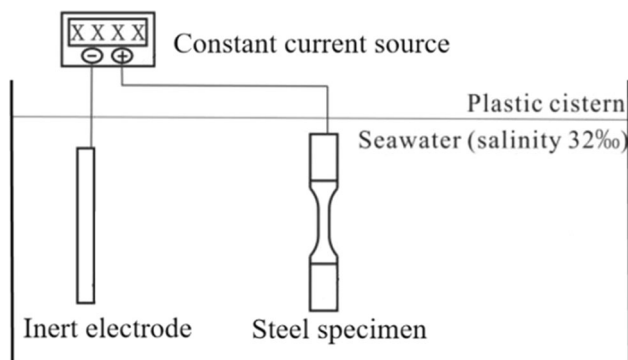


Fig. 3 Electrochemical corrosion test

uneven, and the corrosion depth is unevenly distributed, which is close to natural random corrosion.

4. Mechanical Performance Test of Corrosion Specimen

4.1 Tensile Test Conditions and Parameters

The CRIMS-SDS-100 electro-hydraulic servo dynamic and static testing machine (see Fig. 6) is used to conduct tensile test on specimens. The data acquisition frequency is 10 Hz, the loading temperature is 32 °C, and the loading rate is 0.48 mm/min. The tensile deformation of the sample was measured with an extensometer. The tensile test process meets the requirements of ASTM standards.

4.2 Time-Varying Corrosion Effect on Generalized Mechanical Properties of Corroded Steel

In the overall structural analysis of the corrosion-damaged platform, the cross-section reduction method is generally used

to simulate the corrosion damage of the platform during modeling. However, the cross-section reduction method is more suitable for simulating uniform corrosion and cannot reflect the effects of random corrosion distribution and stress concentration caused by local corrosion. To reflect the above influence, solid modeling or multi-scale modeling is required. This modeling method requires a lot of preliminary modeling work or requires a combination of more difficult programming work. At the same time, due to the large amount of calculation and poor convergence control of this method, the ideal calculation results are difficult to obtain. Another method is to give a generalized constitutive model of steel considering the effect of corrosion in structural modeling to reflect the effect of corrosion damage. Figure 7 shows the nominal stress–strain curves of different corrosion times obtained according to the corrosion cross-sectional area of specimens; it is found that corrosion has little effect on the nominal stress–strain curves of steel. Because the stress–strain relationship of steel is an inherent characteristic of the material and does not change due to corrosion damage, the above-mentioned idea cannot be realized through the nominal stress–strain relationship of steel. Therefore, when calculating the stress–strain relationship of the steel based on the test results, the original cross-sectional area of the corrosion test piece is used.






The stress and strain are defined as follows:

$$\varepsilon = \frac{\Delta l}{l_0} \quad (\text{Eq 2})$$

$$\sigma = \frac{F}{A_0} \quad (\text{Eq 3})$$

where σ and ε are the generalized stress and strain of steel, respectively. l_0 is the initial length of the test section of the specimen. Δl is the elongation of the test section of the specimen. F is the tensile load. A_0 is the initial cross-sectional area of the test section of the specimen. Using this method, the generalized stress–strain curves of the specimens with different

Table 3 Corrosion specimen parameters and photographs

Corrosion time, h	Specimen photographs	Uniform thickness after corrosion, mm	Corrosion thickness reduction rate, %	Corresponding service life, year
1		9.71	2.90	2.97
2		9.58	4.20	3.92
3		9.37	6.30	5.43
5		9.05	9.50	7.91
8		8.35	16.50	18.80

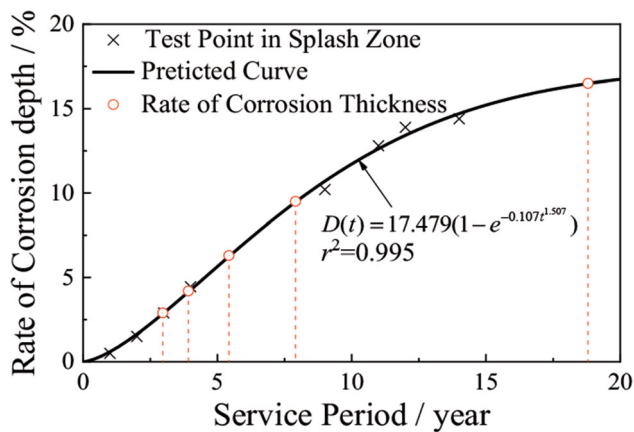


Fig. 4 The regression corrosion curve

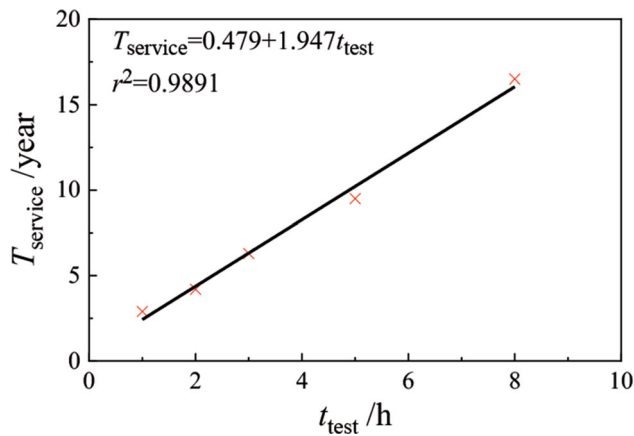


Fig. 5 Correlation between laboratory corrosion thickness and actual corrosion years

corrosion times are obtained, as shown in Fig. 8. This generalized stress–strain relationship reflects the influence of different degrees of corrosion, comparing the curves, it can be

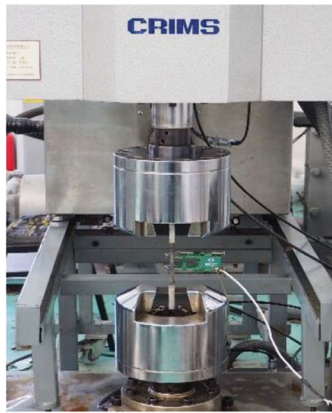
seen that as the corrosion time increases, the yield step of the generalized stress–strain curve is gradually shortened, and the yield strength, ultimate strength and fracture strain decrease. Introducing the relationship between the laboratory corrosion time and the actual corrosion years, the annual variation law of the generalized tensile mechanical characteristic parameters of steel can be further obtained. It can be seen from the figure that the four main characteristic parameters all decrease with the increase of service life. In order to compare the change law of the mechanical characteristic parameters with the annual growth, the characteristic parameters were normalized and regression analyzed, as Fig. 9 shows. It can be seen from Fig. 9 that the yield strength and ultimate strength degrade the most rapidly with corrosion years, followed by the elastic modulus, and the degeneration of ultimate deformation is smaller.

5. Steel Mechanics Model Influenced by Time-Varying Corrosion Effect

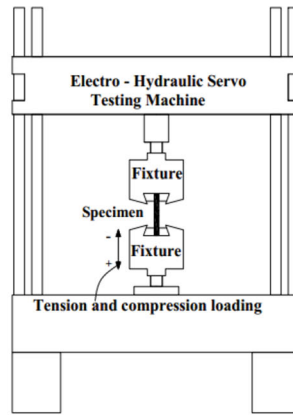
5.1 Regression of Generalized Constitutive Model of Corroded Steel

In order to further obtain the mechanical properties of the corrosion-damaged steel and use it in the overall analysis of the corrosion-damaged platform, a constitutive model of the corrosion-damaged steel was established based on the test data regression. A linear model $\sigma = E\varepsilon$ is used to perform regression analysis on the elastic section of the steel stress–strain curve. At the same time, in order to better simulate the inelastic section of the steel stress–strain curve, and considering that the tensile elongation occupies a small proportion in the strain hardening section, the elastic strain is ignored. The modified R–O model is used to characterize the strain hardening section of the generalized stress–strain curve of steel under different thickness reductions (Ref 16, 21).

$$\sigma = E \left(\frac{\varepsilon}{K} \right)^{\frac{1}{n}} \quad (\text{Eq 4})$$



(a) Physical drawing of testing machine



(b) Schematic diagram of testing machine

Fig. 6 An electro-hydraulic testing machine

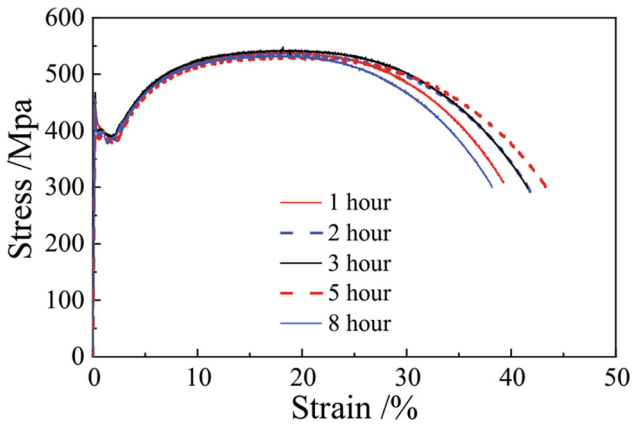


Fig. 7 Stress–strain curve obtained from corrosion cross-sectional area

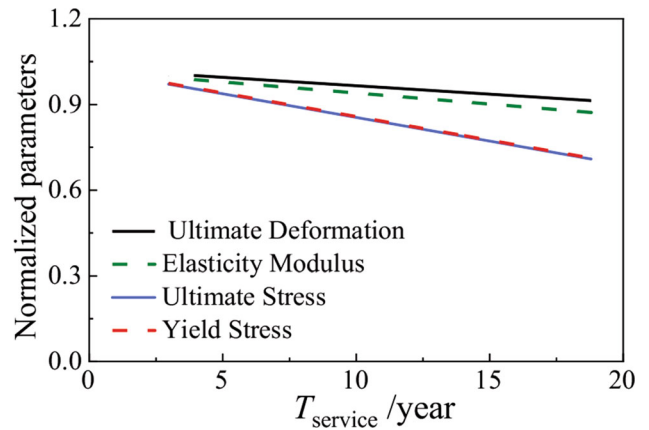


Fig. 9 Normalized comparison of annual variation of mechanical characteristic parameters

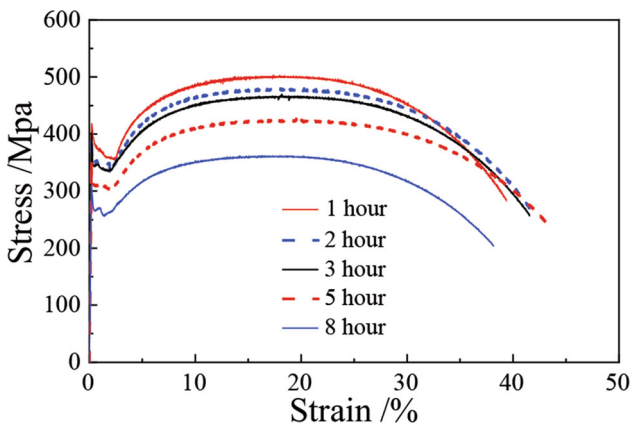


Fig. 8 Stress–strain curve obtained from the original cross-sectional area

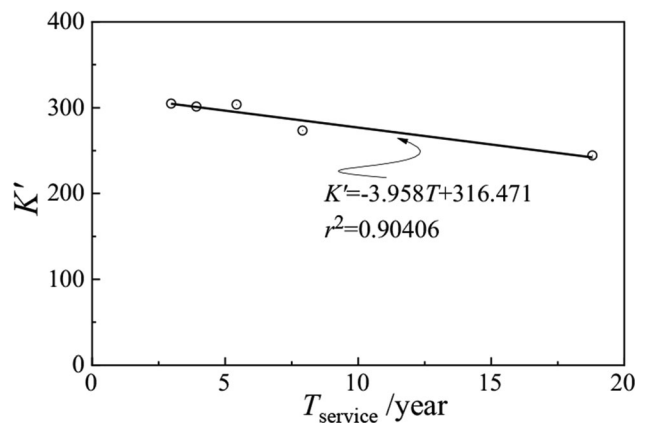


Fig. 10 The relationship between K' and T

where K is the intensity correlation coefficient; n is the index parameter, expressing as strain hardening effect. Both K and n depend on material properties.

Assigning $n' = \frac{1}{n}$, $K' = \frac{E}{K^n}$ the formula can be expressed as:

$$\sigma = K' \varepsilon^{n'} \quad (\text{Eq } 5)$$

N' and K' can be obtained by regression of experimental data, as shown in Fig. 10 and 11. It can be seen from Fig. 10 that the coefficient K' is more sensitive to corrosion thickness reduction, while the coefficient n' does not change much and can be regarded as a constant. Figure 12 shows the steel linear exponential generalized stress–strain model obtained by the

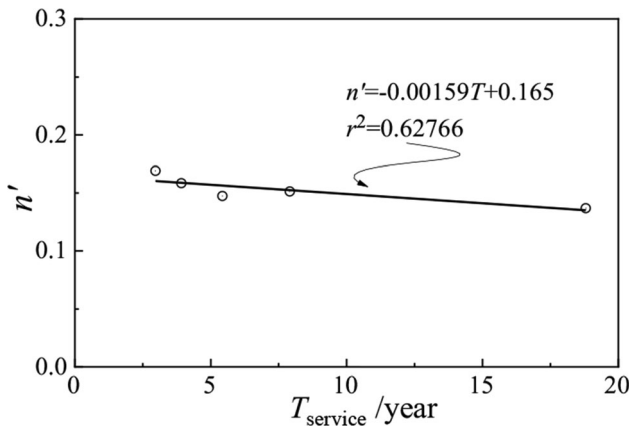


Fig. 11 The relationship between n' and T

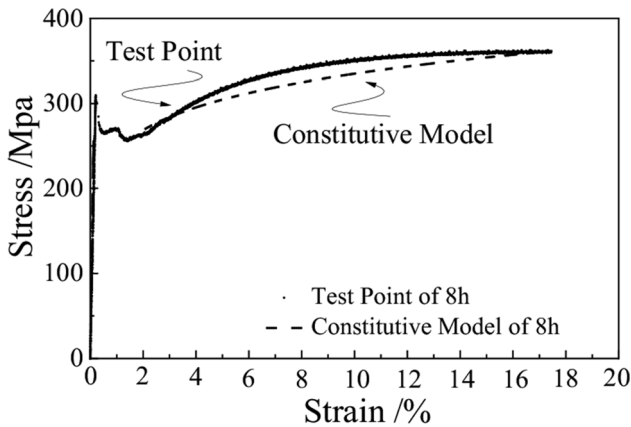


Fig. 12 Comparison of test results with constitutive model

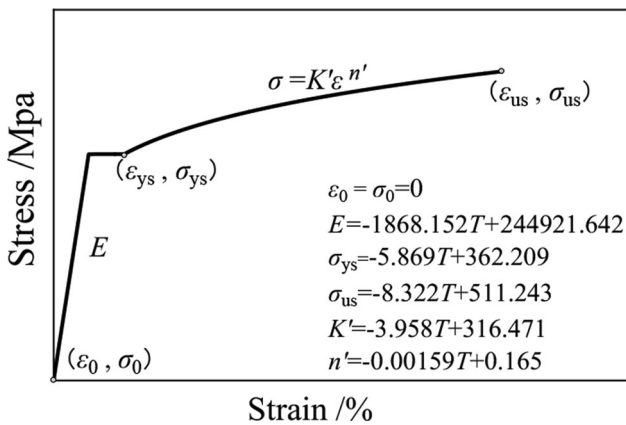


Fig. 13 Generalized constitutive model of corroded steel

above analysis and regression. When the linear exponential model is used for structural analysis, it is conservative.

5.2 Time-Varying Corrosion Law of Corroded Steel Constitutive Model

According to the analysis process of Sect. 5.1, the constitutive model of corroded steel can be obtained, as shown in Fig. 13. The formula in the figure is the expression of each stage of the model. E , σ_{ys} and σ_{us} are the mechanical

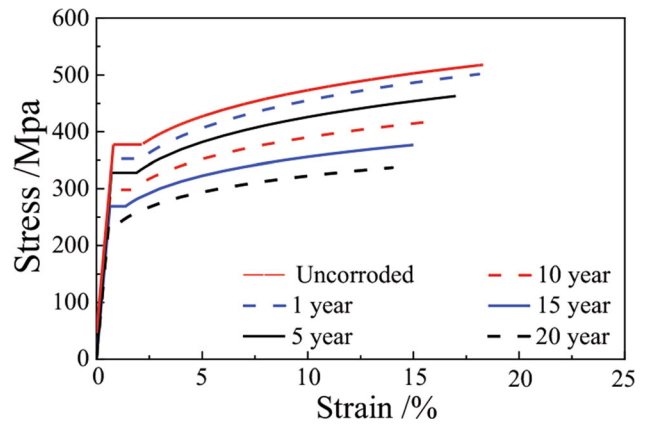


Fig. 14 A constitutive model of steel affected by time-varying corrosion effects

characteristic parameters of steel, which change with the service life. The expressions of E , σ_{ys} and σ_{us} with the service life as the variable can be obtained by regression analysis, and the regression analysis results are shown in Fig. 9. With the help of the model in Fig. 13, the generalized modified constitutive model of steel with different service life can be obtained by changing T . In order to obtain the comparison of the steel constitutive model with the interval service age, the steel constitutive models with the service life of 0 year, 1 year, 5 years, 10 years, 15 years and 20 years are drawn, respectively, as shown in Fig. 14.

6. Analysis of the Overall Performance of the Corrosion Platform

The constitutive model of steel damaged by time-varying corrosion is introduced into the overall structure analysis of the platform to investigate the influence of time-varying corrosion damage on the overall mechanical properties of the platform. To compare with the relevant research results, the jacket offshore platform shown in Yang et al. (Ref 13) (see Fig. 15) is still taken as an example to study the influence of different corrosion damage simulation methods on the overall structural mechanical properties of the platform. The platform is located in the Bohai Sea, and the environmental conditions are consistent with those of the Bohai No. 8 platform. The seismic fortification intensity I is 8 degrees (Ref 22), the recurrence period of the earthquake is 1000 years, the total height of the platform structure is 54 m, and the water depth is 36 m. The foundation of the platform is a four-legged pile structure, the total mass of the platform is 2.995×10^6 kg, the total mass of the upper structure is 2.575×10^6 kg, and the total mass of the jacket part is 0.420×10^6 kg. The basic parameters of the steel used for the platform are as follows: the yield strength is 235 MPa, the Young's modulus is 2.10×10^5 MPa, the Poisson's ratio is 0.3, and the density is 7.85×10^3 kg/m³. The jacket part is composed of pile legs, horizontal braces and diagonal braces, the three components are round tubes, whose section diameter and thickness are 1.2 m and 0.03 m, 0.78 m and 0.025 m, and 0.508 m and 0.02 m in turn.

The basic period of the platform structure (T) is 1.139 s, and the venue type is Category C venue. Through the correspond-

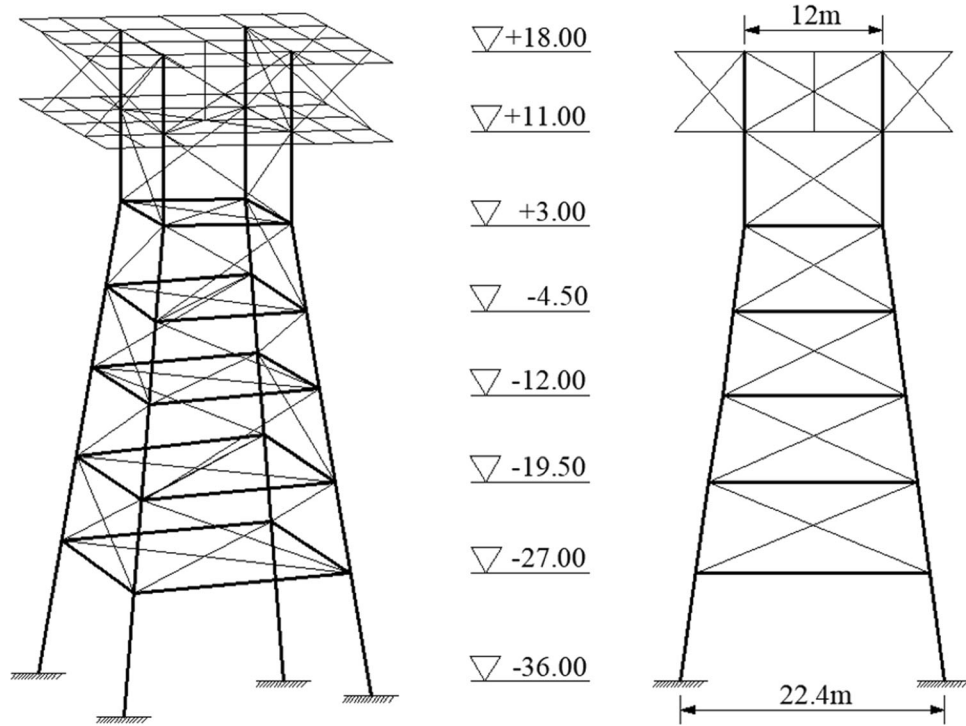


Fig. 15 Schematic of a jacketed offshore platform (Ref 13)

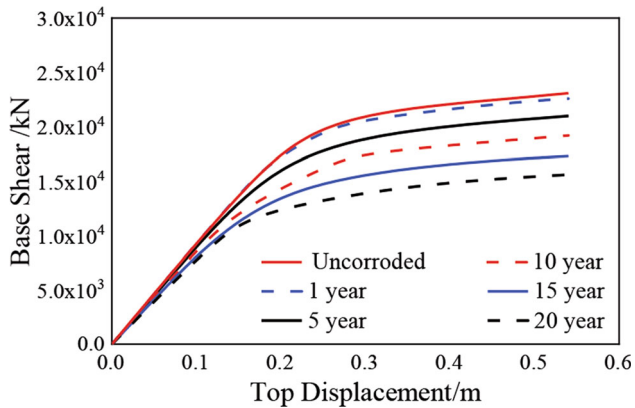


Fig. 16 Pushover curves of platforms with different corrosion years

ing design spectrum of this type of venue, the amplification factor β corresponding to the basic period of 1.139 s can be calculated, that is, $\beta = 1.575/T = 1.575/1.139 = 1.38$ (Ref 13, 22). According to the requirements of the design specification (Ref 22), it is assumed that the bottom of the platform is 6 times the pile diameter below the mud surface as a three-way hinged support. The pile diameter of the platform is 1.2 m; therefore, the hinge support position is 7.2 m below the mud surface. The impact of initial defects was not considered in the analysis. Only one finite element model for the example platform are established. Six kinds of generalized constitutive models are used to consider the corrosion cases (up to 20-year service period).

The reserve strength ratio (RSR) and ductility coefficient (μ) are both required to evaluate the performance of an overall platform in API, CCS, and ISO (Ref 23-25). RSR and μ are calculated by static pushover analysis of the jacket platform.

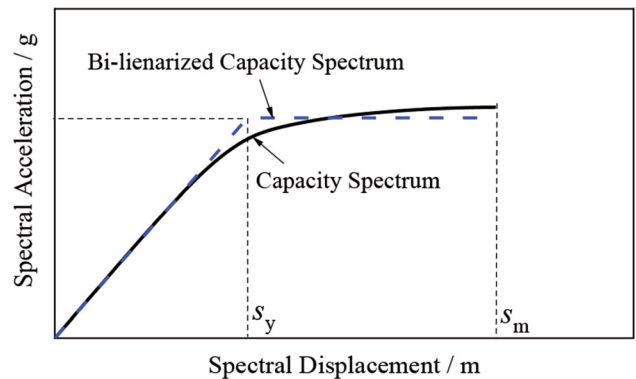


Fig. 17 The capacity spectrum and bi-linearized equivalent capacity spectrum curves

Select the inverted triangle to distribute the lateral force for static pushover analysis. The laterally distributed loads with the constant distribution pattern determined by the fundamental mode of the platform are applied at each floor of the platform in the pushover analysis. The lateral load of each floor follows the ratio determined by $(m_i \times \phi_{i1}) / (\sum m_i \times \phi_{i1})$ in Yang et al. (Ref 13), where the number of floors is 8. In the pushover analysis, the lateral load of each floor is increased in the same proportion until the platform collapses. Figure 16 shows the relationship curves, obtained from the pushover analysis, between base shear and top-displacement of the platform for different service periods. The ultimate capacity of the un-corroded platform, V_u , as indicated by the peak point in Fig. 16, is 2.31×10^4 kN. The design capacity, V_d , is calculated as 1.022×10^4 kN by $V_d = M_1^* \beta A$ (Ref 13). The RSR of the non-corroded platform is $RSR = V_u/V_d = 2.26$. In addition to calculating the strength reserve index of the platform structure, the ductility index of the

structure is also studied. The capacity spectrum curve is

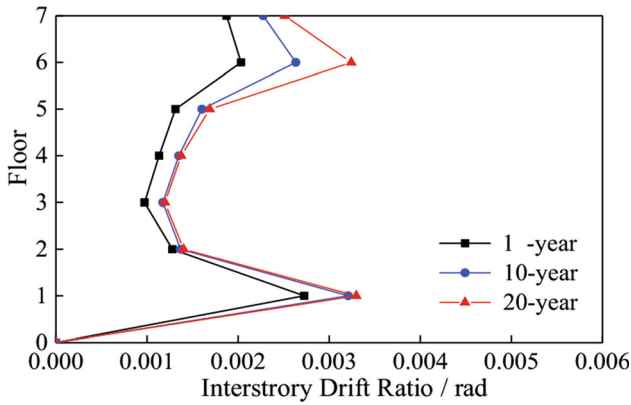


Fig. 18 The inter-layer drift ratios of platforms with different service years

converted into a bi-linearized curve according to the principle of equal energy (Ref 26), and the area enclosed by the capacity spectrum curve and bi-linearized equivalent capacity spectrum curve is required to be approximately equal to that of the axis within the error range. The capacity spectrum and bi-linearized equivalent capacity spectrum curves of the design structure are shown in Fig. 17. The ductility coefficient of the structure can be expressed as $\mu = S_m/S_y$, where S_m is the spectrum displacement of collapse point; S_y is the spectrum displacement of yield point. The μ of the non-corroded platform is $\mu = S_m/S_y = 6.05$.

Obviously, corrosion damage will reduce the carrying capacity of the platform structure. As the corrosion years increase, the ultimate strength of the platform decreases, the deformation increases, the reduction rate of the platform's bearing capacity gradually accelerates, and the risk of damage increases. From the pushover curve (Fig. 16) of the corrosion platform, we can see the changes in the base shear force, the displacement angle between layers, the yield displacement and the ultimate displacement. Such decrease can be attributed to two facts. In addition to the aggressive environmental conditions of the No.8 Bohai platform adopted for the example platform, there is also the sensitivity of the shear strength of the base to the location where corrosion occurs. From the Inter-layer drift ratios of the platform with different corrosion years (see Fig. 18), it can be seen that the sixth layer of the platform is more sensitive to corrosion. After the service period increases, the deformation of the structure at this position is the largest, under the maximum corrosion damage, the inter-layer drift ratios of the sixth layer of the platform increases by 34.4% and becomes the weak layer of the structure. Since the main mass of the platform is concentrated in the upper deck structure, once any structure underneath is damaged, the structure will collapse or overturn due to the $P\Delta$ effect. Figure 19 shows the RSR and μ of the platforms with different service periods. With the increase of corrosion year, RSR and μ show linear changes, the strength reserve capacity of the platform is greatly attenuated, and the ductility reserve capacity does not change much.

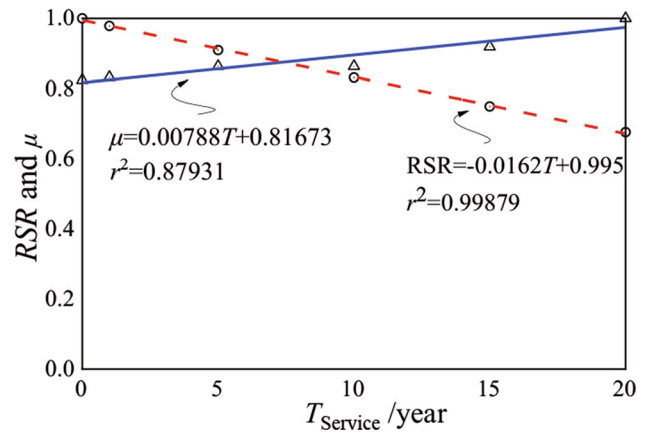


Fig. 19 The change law of platform RSR and μ

7. Conclusion

Corrosion of steel offshore platforms is inevitable. The cross-section reduction method and the solid-multi-scale modeling method have their own defects in simulating the macroscopic behavior of offshore structures with corroded components. Therefore, this paper proposes a time-varying corrosion generalized constitutive model, which can be used to evaluate the mechanical properties of the overall structure of jacket offshore platforms based on the theoretical method and measured data. The main conclusions from this paper are as follows:

1. According to the corrosion monitoring data of the Bohai No. 8 platform during its 18-year service period, the time-varying corrosion depth model of steel in the platform splash zone is obtained. Combined with the change law of the corrosion thickness of the steel in the laboratory, the corresponding relationship between the corrosion of the steel in the laboratory and the actual service year is established.
2. Tensile tests were carried out on steel specimens with different corrosion years, and the time-varying corrosion influence law of steel mechanical properties was obtained. As the degree of corrosion deepens, the generalized mechanical properties of steel degrade to varying degrees. The yield strength, ultimate strength and ductile deformation ability of steel are greatly degraded. According to the above-mentioned change law of mechanical parameters of steel, based on R-O model, a generalized constitutive model of corroded steel with service year as a variable was established.
3. The modified generalized constitutive model of steel corrosion was introduced to simulate the corrosion effects of the platform in different service periods. The static push-over analysis of the platform during the service period of 0-20 years was carried out, and it was found that with the increase of service life, the sixth layer of the platform was more sensitive to corrosion, the structural deformation at this position was the largest, the strength reserve capacity of the platform is greatly attenuated, and the ductility reserve capacity does not change much.

Acknowledgments

This research was financially supported by the National Natural Science Foundation of China (Grant No. 51979036).

References

1. R.E. Melchers, Optimality-Criteria-Based Probabilistic Structural Design, *Struct. Multidiscip. Optim.*, 2001, **23**(1), p 34–39.
2. A. Valor, F. Caleyó, L. Alfonso, D. Rivas, and J. Hallen, Stochastic Modeling of Pitting Corrosion: A New Model for Initiation and Growth of Multiple Corrosion Pits, *Corros. Sci.*, 2007, **49**(2), p 559–579.
3. J. Paik, J. Lee, and M. Ko, Ultimate Shear Strength of Plate Elements with Pit Corrosion Wastage, *Thin-Walled Struct.*, 2004, **42**(8), p 1161–1176.
4. A. Rahbar-Ranji, Ultimate Strength of Corroded Steel Plates with Irregular Surfaces under In-Plane Compression, *Ocean Eng.*, 2012, **54**, p 261–269.
5. S. Qin, W. Cui, and K. Shen, A Non-Linear Corrosion Model for Time Variant Reliability Analysis of Ship Structures, *J. Ship Mech.*, 2003, **7**(1), p 94–103. **(in Chinese)**
6. C. Southwell, J. Bultman, and A. Hummer Jr., Estimating of Service Period of Steel in Seawater, *Seawater Corrosion Handbook*. M. Schumacher Ed., Noyes Data Corporation, NJ, 1979
7. C.G. Soares and Y. Garbatov, Reliability of Maintained Ship Hull Girders Subjected to Corrosion and Fatigue, *Struct. Saf.*, 1998, **20**(3), p 201–219.
8. J. Paik, S. Kim, and K. Sang, Probabilistic Corrosion Rate Estimation Model for Longitudinal Strength Members of Bulk Carriers, *Ocean Eng.*, 1998, **25**(10), p 837–860.
9. Y. Bai, Y.H. Kim, H.B. Yan, X.F. Song, and H. Jiang, Reassessment of the Jacket Structure Due to Uniform Corrosion Damage, *Ship Offshore Struct.*, 2016, **11**(1), p 105–112.
10. R.E. Melchers, The Effect of Corrosion on the Structural Reliability of Steel Offshore Structures, *Corros. Sci.*, 2005, **47**(10), p 2391–2410.
11. Z. Jia, Y. Yang, Z. He, H. Ma, and F. Ji, Mechanical Test Study on Corroded Marine High Performance Steel under Cyclic Loading, *Appl. Ocean Res.*, 2019, **93**, 101942
12. H. Ma, Y. Yang, and Z. Jia, Experimental Study on Tensile Properties of High Strength Marine Steel NV-D36 with Pitting Corrosion, *J. Harbin Eng. Univ.*, 2018, **39**(8), p 1283–1289.
13. Y. Yang, Q. Wu, Z. He, Z. Jia, and X. Zhang, Seismic Collapse Performance of Jacket Offshore Platforms with Time-Variant Zonal Corrosion Model, *Appl. Ocean Res.*, 2019, **84**, p 268–278.
14. G. Soares, Y. Garbatov, and A. Zayed, Effect of Environmental Factors on Steel Plate Corrosion under Marine Immersion Conditions, *Corros. Eng. Sci. Technol.*, 2011, **46**(4), p 524–541.
15. Y. Garbatov, G. Soares, J. Parunov, and J. Kodvanj, Tensile Strength Assessment of Corroded Small Scale Specimens, *Corros. Sci.*, 2014, **85**, p 296–303.
16. W. Ramberg and W. Osgood, Description of Stress–Strain Curves by Three Parameters, Washington: National Advisory Committee for Aeronautics Technical Note. TN 902, 1943
17. B. Kato, Deformation Capacity of Steel Structures, *J. Constr. Steel Res.*, 1990, **17**(1–2), p 33–94.
18. A. Esmaeily and Y. Xiao, Behavior of Reinforced Concrete Columns under Variable Axial Loads: Analysis, *ACI Struct. J.*, 2005, **102**(5), p 736–744.
19. ASTM E 8M-04, Standard Test Methods for Tension Testing of Metallic Materials, ASTM International, West Conshohocken (2012)
20. D. Zhao, Y. Yang, Q. Lu, Z. He, Y. Liu, and L. Zhou, The Effect of Corrosion on the Hysteresis Properties of Welded Steel, *Ship Offshore Struct.*, 2022, **18**(1), p 105–119.
21. Y. Yao, Y. Yang, Z. He, and Y. Wang, Experimental Study on Generalized Constitutive Model of Hull Structural Plate with Multi-parameter Pitting Corrosion, *Ocean Eng.*, 2018, **170**, p 407–415.
22. SY/T 4084-95, Technical Specification of Environmental Conditions and Load in Beach-Shallow Sea. China National Petroleum Corporation. Petroleum Industry Press, Beijing, 1995 **(in Chinese)**
23. American Petroleum Institute (API), Recommended Practice for Planning, Designing and Constructing Fixed Offshore Platforms—Working Stress Design: API Recommended Practice 2A-WSD (the 21st edition). American Petroleum Institute, Washington, DC, 2012
24. China Classification Society (CCS), Rules for the Classification and Construction of Fixed Offshore Platforms. China Classification Society. Beijing People's Traffic Press, Beijing, 1992 **(in Chinese)**
25. International Organization for Standardization (ISO), Petroleum and Natural Gas Industries—Specific Requirements for Offshore Structures—Part 2: Seismic Design Procedures and Criteria, 2006
26. FEMA 273, NEHRP Guidelines for the Seismic Rehabilitation of Buildings. Issued by FEMA in Furtherance of the Decade for Natural Disaster Reduction. Washington DC, Federal Emergency Management Agency, 1997

Publisher's Note Springer Nature remains neutral with regard to jurisdictional claims in published maps and institutional affiliations.

Springer Nature or its licensor (e.g. a society or other partner) holds exclusive rights to this article under a publishing agreement with the author(s) or other rightsholder(s); author self-archiving of the accepted manuscript version of this article is solely governed by the terms of such publishing agreement and applicable law.